ЖЭТФ, 2013, том 144, вып. 1 (7), стр. 60–74

ANALYSIS OF TRIPLET PRODUCTION BY A CIRCULARLY POLARIZED PHOTON AT HIGH ENERGIES

G. I. Gakh, M. I. Konchatnij, I. S. Levandovsky, N. P. Merenkov *

Kharkov Institute of Physics and Technology
61108, Kharkov, Ukraine

Received October 4, 2012

The possibility in principle of determining the circular polarization of a high-energy photon by measuring the created electron polarization in the process of triplet photoproduction $\gamma + e^- \to e^+e^- + e^-$ is investigated. The respective event number, which depends on polarization states of the photon and the created electron, does not decrease as the photon energy increases, and this circumstance can ensure the high efficiency in such experiments. We study different double and single distributions of the created electron (or positron), which allow probing the photon circular polarization and measuring its magnitude (the Stokes parameter ξ_2) using the technique of Sudakov variables. Some experimental setups with different rules for event selection are studied and the corresponding numerical estimations are presented.

DOI: 10.7868/S0044451013070067

1. INTRODUCTION

It is well known that the process of triplet production

$$\gamma(k) + e^-(p) \to e^-(k_1) + e^+(k_2) + e^-(p_1) \qquad (1)$$

by high-energy photons on atomic electrons can be used to measure the photon linear polarization degree [1–3]. This possibility arises due to the azimuthal asymmetry of the corresponding cross section, i. e., due to its dependence on the angle between the plane in which the photon is polarized and the plane $(\mathbf{k}, \mathbf{p}_1)$ where the recoil electron 3-momentum lies. The detailed description of the various differential distributions, such as the dependence on the momentum value, on the polar angle and the minimal recorded momentum of the recoil electron, on the invariant mass of the created electron–positron pair, on the positron energy, and others, was investigated in Ref. [4]. This single-spin effect is the theoretical background of polarimeters, where different angular and energy distributions are used [5].

The exact expressions for differential and partly integrated cross sections of process (1) are very cumbersome and exist in the complete form only in the unpolarized case [6]. At a high collision energy, only two (from eight) diagrams contribute with the leading accuracy (neglecting terms of the order of m^2/s, where $s = 2(kp)$ and m is the electron mass) and the corresponding expressions are essentially simplified. These diagrams (the so-called Borselino diagrams [7]) are shown in Fig. 1. Nevertheless, at the boundaries of the final-particle phase space, the nonleading terms can be enhanced, and some of such effects were investigated in Ref. [8] in the case of linearly polarized photons.

As regards the photon circular polarization, it can be probed by double-spin effects at least. In the region of small and intermediate photon energies, the circular polarization can be measured using double-spin correlation in Compton scattering. For example, in Ref. [9], the corresponding possibility was considered for the Compton cross section asymmetry in the scattering of a photon on polarized electrons. In principle, the polarization of the recoil electron can also be measured. The double-spin effects can be used to create polarized electron beams using laser photons [10].

At high energies of photon beams, the use of Compton scattering is not effective because the Compton cross section decreases very fast as the photon energy increases. If the photon energy is large, the cross section of the electron–positron pair production, which does not decrease as the energy increases, becomes larger than the Compton scattering one. To estimate the relevant energy, we can use the asymptotic formulas

*E-mail: merenkov@kipt.kharkov.ua

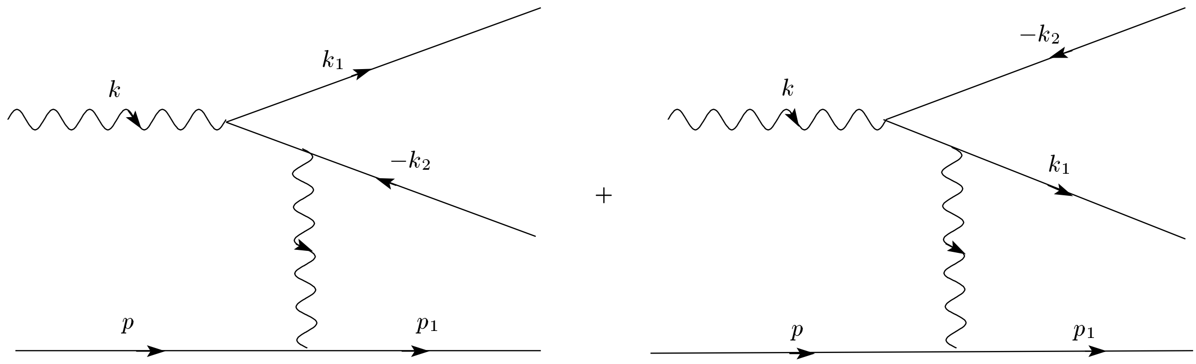

Fig. 1. Borselino diagrams that make a nondecreasing contribution to the cross section at high energies and small transferred momenta

for the total cross sections [11]

$$\sigma_C \approx \frac{2\pi r_0^2}{x}\ln x, \quad \sigma_{pair} \approx \frac{28\alpha r_0^2}{9}\ln x, \tag{2}$$

$$x = \frac{s}{m^2}, \quad \alpha = \frac{1}{137},$$

where $r_0 = \alpha/m$ is the classical radius of the electron. In the rest frame of the initial electron ($s = 2\omega m$), the photon energy ω has to be larger than about 80 MeV. Hence, to measure the circular polarization of photons with the energies more than 100 MeV, it is advantageous to use process (1) rather than the Compton scattering.

The above estimate of the pair production cross section is made taking only the Borselino diagrams into account. The events described by these diagrams have very specific kinematics in the rest frame of the initial electron, namely, the recoil electron has a small 3-momentum (of the order of m), whereas the created electron–positron pair carries all the photon energy and moves along the photon momentum direction. In the reaction c.m.s., the scattered (recoil) electron has a small perpendicular momentum transfer (of the order of m) and a very small longitudinal one (of the order of m^3/s). Just such events contribute to the nondecreasing cross section. The contribution of the other diagrams, describing the direct capture of the photon by the initial electron and exchange effects due to the identity of the final electrons, decreases at least as m/ω.

There are a few possibilities to measure the photon circular polarization in process (1): i) to use longitudinally polarized electrons and measure the asymmetry of the cross section at two opposite directions of the polarization, ii) to measure the polarization of recoil electrons, iii) to measure the polarization of the created electrons or positrons. The double-spin correlation effects in the first two cases decrease as the photon energy increases, and are not therefore effective for measuring the photon circular polarization at high energies. In this paper, we therefore concentrate on the third experimental setup, which can be realized in the scattering of photons on unpolarized atomic electrons or an electron beam. In some aspects, our study is close to the approach in Ref. [12], where process (1) with circularly polarized photons was suggested to create high-energy polarized electrons; in the last section, we discuss the corresponding similarities and differences in more detail.

2. FOUR-RANK COMPTON TENSOR

In the approximation considered here, the squared matrix element of process (1) is defined by a contraction of two second-rank Lorentz tensors $V_{\mu\nu}$ and $B_{\mu\nu}$, and the differential cross section of this process can be written in the form

$$d\sigma = \frac{e^6}{2(2\pi)^5 s q^4} V_{\mu\nu} B_{\mu\nu} d\Phi, \tag{3}$$

$$d\Phi = \frac{d^3k_1}{2E_1}\frac{d^3k_2}{2E_2}\frac{d^3p_1}{2\varepsilon_1}\delta(k + p - p_1 - k_1 - k_2),$$

where $q = k - k_1 - k_2 = p_1 - p$, E_1 (E_2) is the energy of the created electron (positron), and ε_1 is the energy of the recoil electron with the 4-momentum p_1. The tensor $B_{\mu\nu}$ is defined by the electron current j_μ,

$$B_{\mu\nu} = j_\mu j_\nu^*, \quad j_\mu = \bar{u}(p_1)\gamma_\mu u(p), \tag{4}$$

and in the case of a polarized initial electron,

$$B_{\mu\nu} = \frac{1}{2}\,\mathrm{Tr}(\hat{p}_1 + m)\gamma_\mu(\hat{p} + m)(1 - \gamma_5\hat{W})\gamma_\nu,$$

where W_μ is its polarization 4-vector. Taking the trace over the spinor indices, we have

$$B_{\mu\nu} = q^2 g_{\mu\nu} + 2(pp_1)_{\mu\nu} - 2im(\mu\nu qW), \qquad (5)$$

where we set

$$(ab)_{\mu\nu} = a_\mu b_\nu + a_\nu b_\mu, \quad (\mu\nu qW) = \epsilon_{\mu\nu\lambda\rho} q_\lambda W_\rho,$$

$$\epsilon_{1230} = 1.$$

If the initial electron is unpolarized and we want to measure the recoil electron polarization, we must substitute

$$p \leftrightarrows p_1, \quad \mu \leftrightarrows \nu, \quad W \to W_1$$

in the right hand side of Eq. (5), which results simply in the change $W \to W_1$, where W_1 is the polarization 4-vector of the recoil electron.

For events with an arbitrarily polarized photon beam, the tensor $V_{\mu\nu}$ in Eq. (3) can be written in terms of its Stokes parameters ξ_i $(i = 1, 2, 3)$ and the four-rank Compton tensor $T_{\mu\nu\lambda\rho}$ (such that its contractions with q_μ, q_ν and k_λ, k_ρ are equal to zero and which is defined below) as

$$V_{\mu\nu} = \frac{1}{2}\big([e_{1\lambda}e_{1\rho} + e_{2\lambda}e_{2\rho}] + \xi_3[e_{1\lambda}e_{1\rho} - e_{2\lambda}e_{2\rho}] + \\ +\xi_1[e_{1\lambda}e_{2\rho}+e_{2\lambda}e_{1\rho}] - i\xi_2[e_{1\lambda}e_{2\rho}-e_{2\lambda}e_{1\rho}]\big)T_{\mu\nu\lambda\rho}, \qquad (6)$$

where the mutually orthogonal space-like 4-vectors e_1 and e_2, relative to which the photon polarization properties are defined, satisfy the relations

$$e_1^2 = e_2^2 = -1, \quad (e_1 k) = (e_2 k) = (e_1 e_2) = 0.$$

The first term inside the parentheses in the right-hand side of Eq. (6) is responsible for the events with an unpolarized photon, the second and third terms are responsible for the events with the linear photon polarization, and the last term, for the events with the circular polarization. The parameters ξ_1 and ξ_3, which define the linear polarization degree of the photon, depend on the choice of the 4-vectors e_1 and e_2, whereas ξ_2 is independent of them. Because we want to investigate events with the circular photon polarization, we can choose these 4-vectors in the most convenient way, namely,

$$e_{1\lambda} = \frac{\chi_1 k_{2\lambda} - \chi_2 k_{1\lambda}}{N}, \quad e_{2\lambda} = \frac{(\lambda\, k\, k_1\, k_2)}{N} \qquad (7)$$

with the short notation

$$N = 2\chi\chi_1\chi_2 - m^2(\chi_1^2 + \chi_2^2),$$

$$\chi_{1,2} = (kk_{1,2}), \quad \chi = (k_1 k_2).$$

The 4-vector e_1 appears in the expression for the fourth-rank Compton tensor $T_{\mu\nu\lambda\rho}$, see Eq. (8) below.

The polarization properties of a real photon are defined by two orthogonal 3-vectors $\mathbf{n_1}$ and $\mathbf{n_2}$. Each of these two vectors is also orthogonal to the photon momentum 3-vector $\mathbf{k}$, and the 4-vectors e_1 and e_2 are their covariant generalizations. It follows from the definition of e_1 and e_2 that they have both time and space components. Adding the 4-vector k with appropriate factors to them (which is, in fact, a gauge transformation), we can eliminate the time and longitudinal (parallel to $\mathbf{k}$) components. In an arbitrary Lorentz system with the z axis directed along the vector $\mathbf{k}$ and the 3-momentum lying in the zx plane, where

$$k = (\omega, 0, 0, \omega), \quad k_1 = (E_1, k_{1x}, 0, k_{1z}),$$

$$k_2 = (E_2, k_{2x}, k_{2y}, k_{2z}),$$

the corresponding transformation has the form

$$(0, \mathbf{n_1}) = e_{1\lambda} - \frac{E_1 k_{2z} - E_2 k_{1z}}{N} k_\lambda,$$

$$(0, \mathbf{n_2}) = e_{1\lambda} - \frac{k_{1x}k_{2y}}{N} k_\lambda,$$

where

$$\mathbf{n_1} = (n_x, n_y, 0), \quad \mathbf{n_2} = (n_y, -n_x, 0),$$

$$n_x = \frac{\omega[(E_1 - k_{1z})k_{2x} - (E_2 - k_{2z})k_{1x}]}{N},$$

$$n_y = \frac{\omega(E_1 - k_{1z})k_{2y}}{N},$$

$$N^2 = \omega^2\big\{[(E_1 - k_{1z})k_{2x} - (E_2 - k_{2z})k_{1x}]^2 + \\ + (E_1 - k_{1z})^2 k_{2y}^2\big\}.$$

Under this transformation, no observables are changed due to the gauge invariance, which manifests itself by means of the above-mentioned constraints on the tensor $T_{\mu\nu\lambda\rho}$,

$$k_\lambda T_{\mu\nu\lambda\rho} = k_\rho T_{\mu\nu\lambda\rho} = 0.$$

That is why the description of all polarization phenomena in process (1) by means of the 4-vectors e_1 and e_2 is completely equivalent to the description in terms of the 3-vectors $\mathbf{n_1}$ and $\mathbf{n_2}$. The evident advantage of the covariant description is the independence from the Lorentz system.

For the events in which the created electron polarization states in process (1) must be determined, the Borselino diagrams lead to the following expression for the tensor $T_{\mu\nu\lambda\rho}$:

$$T_{\mu\nu\lambda\rho} = \frac{1}{2}\,\mathrm{Tr}\,\{(\hat{k_1}+m)(1-\gamma_5\hat{S})\times \\ \times \hat{Q}_{\lambda\mu}(\hat{k_2}-m)\hat{Q}_{\nu\rho}\}, \qquad (8)$$
$$\hat{Q}_{\lambda\mu} = \frac{N}{\chi_1\chi_2}e_{1\lambda}\gamma_\mu + \frac{\gamma_\lambda\hat{k}\gamma_\mu}{2\chi_1} - \frac{\gamma_\mu\hat{k}\gamma_\lambda}{2\chi_2},$$

where S is the electron spin 4-vector, with the properties $S^2=-1$ and $(Sk_1)=0$.

We divide $T_{\mu\nu\lambda\rho}$ into two parts: the first part depends on the 4-vector S and the second one does not,

$$T_{\mu\nu\lambda\rho} = T^{(S)}_{\mu\nu\lambda\rho} + T^{(0)}_{\mu\nu\lambda\rho}.$$

Then we can write

$$T^{(0)}_{\mu\nu\lambda\rho} = T_{(\mu\nu)(\lambda\rho)} + T_{[\mu\nu][\lambda\rho]}, \\ T^{(S)}_{\mu\nu\lambda\rho} = im\big[T_{(\mu\nu)[\lambda\rho]} + T_{[\mu\nu](\lambda\rho)}\big], \qquad (9)$$

where we use the index notation $(\alpha\beta)$ ($[\alpha\beta]$) to indicate the symmetry (antisymmetry) under the permutation of indices α and β. These symmetry properties (9) and form (5) for the tensor $B_{\mu\nu}$ allow discussing some features of process (1) with a high-energy polarized photon on the qualitative level.

As noted in the Introduction, the cross section of process (1) (when all particles are unpolarized) does not decrease as the photon energy increases. Such behavior is caused by terms proportional to s^2 in the contraction $T_{\mu\nu\lambda\rho}B_{\mu\nu}$ that enters differential cross section (3). On the other hand, only the symmetric component $2(pp_1)_{\mu\nu}$ in Eq. (5) can ensure the appearance of such terms. This simple observation suggests that the nondecreasing spin correlations in the differential cross section in the considered case are connected only with the tensors $T_{(\mu\nu)(\lambda\rho)}$ and $T_{(\mu\nu)[\lambda\rho]}$ that are symmetric under the $\mu \leftrightarrows \nu$ permutation. The first one describes single-spin correlations that depend on Stokes parameters ξ_1 and ξ_3 caused by the linear photon polarization [1]. The second tensor can contribute under the condition that the polarization of the created electron (or positron) is measured, or in other words, it describes double-spin correlation dependent on Stokes parameter ξ_2 that is the circular polarization degree. In what follows, we concentrate just on this double-spin correlation, which can be used to measure the ξ_2 parameter.

The tensors $T_{[\mu\nu][\lambda\rho]}$ and $T_{[\mu\nu](\lambda\rho)}$ that are antisymmetric under the $\mu \leftrightarrows \nu$ permutation do not have much physical significance in the considered problem because they can describe spin correlations in differential cross sections that decrease at least as s^{-1} with the increase in energy. For the full description in such an approximation, it is not enough to consider only the Borselino diagrams, and the other six diagrams must be taken into account. But these tensors are connected by the cross symmetry with the corresponding tensors in the annihilation channel that are suitable for the description of the subprocess $e^+ + e^- \to \gamma + \gamma^*$, which is important in different radiative return measurements [13] and which does not acquire contributions of any other diagrams. That is why we give all the corresponding expressions in very compact form

$$T_{(\mu\nu)(\lambda\rho)} = \frac{2}{\chi_1\chi_2}\times \\ \times\Big\{g_{\mu\nu}\Big[(\chi_1+\chi_2)^2 g_{\lambda\rho} - \frac{N^2}{\chi_1\chi_2}\,q^2\,e_{1\lambda}e_{1\rho}\Big] - \\ - 2\chi_1\chi_2(1+\hat{P}_{\lambda\rho})\,g_{\mu\rho}g_{\nu\lambda} - 2(k_1k_2)_{\lambda\rho}k_\mu k_\nu + \\ + \big(1+\hat{P}_{\lambda\rho}+\hat{P}_{\mu\nu}+\hat{P}_{\lambda\rho}\hat{P}_{\mu\nu}\big)g_{\nu\rho}\big[k_\mu(\chi_2k_{1\lambda}+\chi_1k_{2\lambda})+ \\ + N(k_{1\mu}-k_{2\mu})e_{1\lambda}\big] + \\ + N\Big[\frac{(k_1e_1)_{\lambda\rho}(kk_2)_{\mu\nu}}{\chi_1} - \frac{(k_2e_1)_{\lambda\rho}(kk_1)_{\mu\nu}}{\chi_2}\Big] - \\ - g_{\lambda\rho}\big[(\chi_1+\chi_2)(k_{12}k)_{\mu\nu} - 2(m^2+\chi)k_\mu k_\nu\big]\Big\}, \qquad (10)$$

where $k_{12} = k_1 + k_2$, $\hat{P}_{\alpha\beta}$ is the $\alpha \rightleftarrows \beta$ permutation operator, and

$$T_{[\mu\nu][\lambda\rho]} = \frac{2}{\chi_1\chi_2}\Big\{(1-\hat{P}_{\mu\nu})\Big[(\chi_1^2+\chi_2^2)g_{\mu\lambda}g_{\nu\rho} + \\ + \frac{(\chi_1^2k_{2\mu}-\chi_2^2k_{1\mu})k_\nu[k_1k_2]_{\lambda\rho}}{\chi_1\chi_2}\Big] + \\ +(1-\hat{P}_{\mu\nu}-\hat{P}_{\lambda\rho}+\hat{P}_{\mu\nu}\hat{P}_{\lambda\rho})\Big[\frac{N}{\chi_1\chi_2}g_{\nu\lambda}e_{1\rho}(\chi_2^2k_{1\mu}-\chi_1^2k_{2\mu})+ \\ + \frac{\chi_1^2-(\chi_1-\chi_2)(m^2+\chi)}{\chi_1}g_{\mu\rho}k_\nu k_{1\lambda} + \\ + \frac{\chi_2^2-(\chi_2-\chi_1)(m^2+\chi)}{\chi_2}g_{\mu\rho}k_\nu k_{2\lambda}\Big]\Big\}, \qquad (11)$$

where we use the notation $[ab]_{\alpha\beta} = a_\alpha b_\beta - a_\beta b_\alpha$.

The spin-dependent parts of $T_{\mu\nu\lambda\rho}$ are given by

$$T_{[\mu\nu](\lambda\rho)} = -2(\mu\nu qS)h_\lambda h_\rho + \\ + \frac{(\mu\nu qk)}{\chi_1^2\chi_2}\big[(\chi_2-\chi_1)(kS)g_{\lambda\rho} - \chi_1\chi_2(Sh)_{\lambda\rho}\big] - \\ - \frac{(kS)}{\chi_1}\big[h_\lambda(\mu\nu\rho q) + h_\rho(\mu\nu\lambda q)\big], \qquad (12)$$

where

$$h = \frac{k_2}{\chi_2} - \frac{k_1}{\chi_1},$$

and

$$T_{(\mu\nu)[\lambda\rho]} = \Big[\frac{(k_1k_1)_{\mu\nu} + (k_2k_2)_{\mu\nu}}{\chi_1\chi_2} - \\ - \Big(\frac{1}{\chi_1^2} + \frac{1}{\chi_2^2}\Big)(k_1k_2)_{\mu\nu} + \\ + \frac{q^2(\chi_1-\chi_2)^2 + \chi_1(\chi_1^2-\chi_2^2)}{2\chi_1^2\chi_2^2}\Big](\lambda\rho kS) + \\ + \frac{(\lambda\rho k k_{12})}{\chi_2}\Big[(Sh)_{\mu\nu} + (Sk_2)\Big(\frac{1}{\chi_1} - \frac{1}{\chi_2}\Big)g_{\mu\nu}\Big] + \\ + \Big\{(\mu\lambda\rho k)\Big[\Big(\frac{(k_2S)}{\chi_2} - \frac{(kS)}{\chi_1}\Big)\Big(\frac{k_{2\nu}}{\chi_1} - \frac{k_{1\nu}}{\chi_2}\Big) + \\ + \frac{(\chi_1-\chi_2)}{2\chi_1\chi_2^2}(q^2 + 2\chi_1 + 2\chi_2)S_\nu\Big] + (\mu \leftrightarrows \nu)\Big\}. \quad (13)$$

3. DIFFERENTIAL CROSS SECTION

When calculating the contribution to the unpolarized part of the cross section that does not decrease as the energy increases, we ought to account for terms proportional to s^2 in the contraction $T_{\mu\nu\lambda\rho}(e_{1\lambda}e_{1\rho}+e_{2\lambda}e_{2\rho})B_{\mu\nu}$, which arise due to the scalar products (k_1p), (k_2p), and (kp). For this, it suffices to use the approximation $B_{\mu\nu} = 4p_\mu p_\nu$ (see Ref. [3]). Then we have

$$T_{\mu\nu\lambda\rho}(e_{1\lambda}e_{1\rho}+e_{2\lambda}e_{2\rho})B_{\mu\nu} = -16\Big[\frac{4m^2}{\chi_1\chi_2}(k_1p)(k_2p) + \\ +(k_1p)^2\Big(\frac{q^2}{\chi_1\chi_2} - \frac{2m^2}{\chi_2^2}\Big) + (k_2p)^2\Big(\frac{q^2}{\chi_1\chi_2} - \frac{2m^2}{\chi_1^2}\Big)\Big]. \quad (14)$$

The leading contribution to the differential cross section, within the chosen accuracy, is given by the region of small transferred momenta $|q^2| \sim m^2$. In this case, it is useful to introduce the so-called Sudakov variables [14], which are suitable for the calculation at high energies and small transferred momenta. These variables, in fact, define a decomposition of the final-state 4-momenta into longitudinal and transverse components relative to the 4-momenta of the initial particles. For process (1), we have (also see [12])

$$k_2 = \alpha p' + \beta k + k_\perp, \quad q = \alpha_q p' + \beta_q k + q_\perp, \\ p' = p - \frac{m^2}{s}k, \quad s = 2(kp), \quad p'^2 = 0, \\ (k_\perp p) = (k_\perp k) = (q_\perp p) = (q_\perp k) = 0, \\ d^4k_2 = \frac{s}{2}d\alpha\, d\beta\, d^2k_\perp, \quad d^4q = \frac{s}{2}d\alpha_q\, d\beta_q\, d^2q_\perp, \quad (15)$$

where the 4-vectors $k_\perp$ and $q_\perp$ are space-like, and hence $k_\perp^2 = -\mathbf{k}^2$, $q_\perp^2 = -\mathbf{q}^2$, and $\mathbf{k}$ and $\mathbf{q}$ are two-dimensional Euclidean vectors.

The phase space of the final particles with the overall δ-function (see Eq. (3)) can be written as

$$d\Phi = \frac{s^2}{4}d\alpha\, d\beta\, d^2k_\perp d\alpha_q d\beta_q d^2q_\perp \times \\ \times \delta(k_2^2 - m^2)\delta(k_1^2 - m^2)\delta(p_1^2 - m^2). \quad (16)$$

Using the conservation laws, we derive

$$k_2^2 = s\alpha\beta - \mathbf{k}^2, \quad k_1^2 = -s(1-\beta)(\alpha+\alpha_q) - (\mathbf{k}+\mathbf{q})^2, \\ p_1^2 = s\beta_q + m^2 - \mathbf{q}^2, \quad s\alpha = \frac{m^2+\mathbf{k}^2}{\beta}, \quad s\beta_q = \mathbf{q}^2, \\ s\alpha_q = -\frac{m^2+\mathbf{k}^2}{\beta} - \frac{m^2 + (\mathbf{k}+\mathbf{q})^2}{1-\beta},$$

and after the integration over α, α_q, and β_q with the help of three δ-functions, the phase space reduces to the very simple expression

$$d\Phi = \frac{1}{4s\beta(1-\beta)}d\beta\, d\mathbf{k}\, d\mathbf{q}. \quad (17)$$

The variable $\beta = E_2/\omega$ is the photon energy fraction that is carried away by the positron (the created electron energy is $E_1 = (1-\beta)\omega$). In terms of the Sudakov variables, the independent invariants are expressed as

$$\chi_1 = \frac{m^2 + (\mathbf{k}+\mathbf{q})^2}{2(1-\beta)}, \quad \chi_2 = \frac{m^2+\mathbf{k}^2}{2\beta}, \\ q^2 = -\mathbf{q}^2 - \frac{m^2(m^2+\mathbf{k}^2)^2}{s^2\beta^2(1-\beta)^2}. \quad (18)$$

In what follows, we consider two possible experimental situations: i) both the scattered (recoil) and created electron are recorded, ii) only the created electron is recorded. In the first case, we assume that events with $|q^2| < |q_0^2|$ are not detected, where the minimal selected momentum transfer squared $|q_0^2|$ is of the order of m^2. In the second case, all events with $|q^2| \geq |q^2_{min}|$ are included, where $|q^2_{min}|$ is the minimal possible value of $|q^2|$, which is defined by the second term in the expression for $-q^2$ in Eq. (18). It is just the longitudinal transferred momentum squared.

These two event selections give very different values for the differential cross section. If $|q^2|$ is of the order of m^2, we can everywhere neglect q^2_{min}. Such a procedure leads to the cross section that depends on q_0, but does not depend on the collision energy (the s invariant). On the other hand, when values of $|q^2|$ for the selected events begin from q^2_{min}, the integration over $d\mathbf{q}$ leads to a logarithmic increase in the corresponding cross section as the collision energy increases. This leading logarithmic contribution can be derived by the equivalent photon method [15], but our goal is to also calculate the next-to-leading (constant) contribution.

We begin with discussing the first experimental setup. Using the definition of the differential cross section (Eq. (3)) and relation (14), taking phase space factor (17) and expressions for independent invariants (18) into account and recalling that

$$2(k_1p) = (1-\beta)s, \quad 2(k_2p) = \beta s, \quad q^2 = -\mathbf{q}^2$$

in the case under study, we obtain

$$d\sigma = \frac{2\alpha^3}{\pi^2\mathbf{q}^4} \times \\ \times \Big[2m^2\beta(1-\beta)\Big(\frac{1}{m^2+(\mathbf{k}+\mathbf{q})^2} - \frac{1}{m^2+\mathbf{k}^2}\Big)^2 + \\ + \frac{\mathbf{q}^2[1-2\beta(1-\beta)]}{[m^2+(\mathbf{k}+\mathbf{q})^2][m^2+\mathbf{k}^2]}\Big] d\beta\, d\mathbf{k}\, d\mathbf{q}. \quad (19)$$

Our goal is to derive the distribution on the electron (positron) energy β and the perpendicular transferred momentum squared ($\mathbf{q}^2$). We therefore have to integrate the right-hand side of Eq. (19) over $d\mathbf{k}$, and the effective values of $|\mathbf{k}|$ are of the order of m. Because the integral rapidly converges, we can take 0 and ∞ as the limits of integration over $|\mathbf{k}|$. After the integration, the differential cross section becomes

$$\frac{d\sigma^l}{d\beta d\mathbf{q}^2} = \frac{4\alpha^3}{\mathbf{q}^4} \times \\ \times\Big\{\big[1-2\beta(1-\beta)\big]\Psi_1 + 2\beta(1-\beta)\Psi_2\Big\}, \\ \Psi_1 = \frac{1}{x}\ln\frac{x+1}{x-1}, \quad \Psi_2 = 1 - \frac{2m^2}{\mathbf{q}^2}\Psi_1, \\ x = \sqrt{1+\frac{4m^2}{\mathbf{q}^2}}. \quad (20)$$

In the limit $\mathbf{q}^2/m^2 \gg 1$, $\Psi_1 = \ln(\mathbf{q}^2/m^2)$ and $\Psi_2 = 1$. In the opposite limit $\mathbf{q}^2/m^2 \ll 1$, the expression in the braces in the right-hand side of Eq. (20) must be proportional to $\mathbf{q}^2$ due to gauge invariance. In this case,

$$\Psi_1 = \frac{\mathbf{q}^2}{2m^2}\left(1-\frac{\mathbf{q}^2}{6m^2}\right), \quad \Psi_2 = \frac{\mathbf{q}^2}{6m^2}.$$

Elementary integration of this cross section over the positron energy fraction β,

$$\frac{d\sigma^l}{d\mathbf{q}^2} = \frac{4\alpha^3}{3\mathbf{q}^4}\left[1+2\left(1-\frac{m^2}{\mathbf{q}^2}\right)\Psi_1\right], \quad (21)$$

allows finding the distribution over the recoil momentum l in the rest frame of the initial electron (formula (16) in Ref. [16]) which is related to $\mathbf{q}^2$ as

$$\mathbf{q}^2 + 2m^2 = 2m\sqrt{m^2+l^2}.$$

This is a test of our calculation. But we do not integrate over β in what follows because we have to keep information about the created pair.

For the pair creation via process (1) by a high-energy photon on a relativistic initial electron with the energy $E \gg m$ in back-to-back collision, the scattered (recoil) electron can be detected, in principle, by means of a circular detector that sums all events with $\theta_{min} < \theta < \theta_{max}$, where the scattering electron angle is $\theta = |\mathbf{q}|/E$. Here, we bear in mind that the scattered electron energy ε_1 is virtually the same as the initial electron energy E. In such an experimental setup, differential cross section (20) is to be integrated over the detector aperture. The maximum and minimum values of $\mathbf{q}^2$ are defined by the angular dimensions of the detector,

$$\mathbf{q}^2_{min} = E^2\theta^2_{min}, \quad \mathbf{q}^2_{max} = E^2\theta^2_{max}.$$

For analytic integration, it is convenient to introduce the new variable $\mathbf{q}^2/m^2 = 4\,\mathrm{sh}^2 z$, whence

$$\Psi_1 = 2z\,\mathrm{th}\, z, \quad \Psi_2 = 1 - \frac{z}{\mathrm{sh}\, z\,\mathrm{ch}\, z}, \quad \frac{d\mathbf{q}^2}{\mathbf{q}^4} = \frac{\mathrm{ch}\, z\, dz}{2m^2\,\mathrm{sh}^3 z},$$

and the integration of Eq. (20) with respect to the azimuthal angle and the new variable z leads to the electron (positron) spectrum in the unpolarized case

$$\frac{d\sigma}{d\beta} = 2\alpha r_0^2\big\{A(z_0) - A(z_1) + \beta(1-\beta) \times \\ \times \big[B(z_0) - B(z_1)\big]\big\}, \quad (22)$$

where z_0 and z_1 are the minimal and maximal values of z, $z = \mathrm{Arsh}(\theta E/2m)$, and

$$A(z) = 2z\,\mathrm{cth}\, z - 2\ln(2\,\mathrm{sh}\, z), \quad (23)$$

$$B(z) = \frac{2}{3\,\mathrm{sh}^2 z} - 2z\,\mathrm{ch}\, z - \frac{2}{3}z\,\mathrm{ch}^3 z + \frac{8}{3}\ln(2\,\mathrm{sh}\, z).$$

We fixed the integration constant such that $A(z)$, $B(z) \to 0$ as $z \to \infty$. This choice is determined by the behavior of cross section (16) at large $\mathbf{q}^2/m^2$.

The total cross section in such an experimental setup can be derived by elementary integration over the positron energy fraction:

$$\sigma = 2\alpha r_0^2\big[C(z_0) - C(z_1)\big], \\ C(z) = A(z) + \frac{1}{6}B(z). \quad (24)$$

We note that in the e^+e^- pair production by a photon on a stationary target with an arbitrary mass M,

$\mathbf{q^2}$ is related to the target mass M and the energy W of the recoil particle in the labaratory system as

$$\mathbf{q^2} = 2M(W - M), \quad W = \sqrt{M^2 + l^2},$$

where l is the absolute value of the recoil momentum. This means that in the case of an atomic electron target, $l = m\,\mathrm{sh}(2z)$, $M = m$, and for a very heavy target, $l = 2m\,\mathrm{sh}(z)$, $M \gg m$. For a stationary target, it is possible to investigate this experimental setup when the detector records all events with $l > l_0$, $l_0 \sim m$. In this case, we can formally set the upper integration limit in Eq. (16) equal to infinity. To write the corresponding results, it suffices to eliminate $A(z_1)$, $B(z_1)$, and $C(z_1)$ from Eqs. (22) and (24).

On the other hand, we can study the angular distribution of the recoil electrons. It is easy to see that in this case, the angle ϑ between the photon 3-momentum and the recoil electron momentum $\mathbf{p_1}$ is defined by the relation [2]

$$\sin^2\vartheta = \frac{4m^2}{4m^2 + \mathbf{q^2}}.$$

It means that large $\mathbf{q^2}$ correspond to small recoil angles ϑ and vice versa. In this case, $\mathrm{sh}\,z = \mathrm{ctg}\,\vartheta$.

We consider the situation where the recoil electron is not detected. In this case, we must integrate over all possible range of the variable $\mathbf{q}^2$, beginning from zero. At very small $\mathbf{q}^2$, such that

$$0 < \mathbf{q}^2 < \sigma, \quad m^6/s^2 \ll \sigma \ll m^2, \tag{25}$$

the differential cross section can be modified by the substitution

$$\mathbf{q}^4 \to \left(\mathbf{q}^2 + \frac{m^2 s_1^2}{s^2}\right)^2, \quad s_1 = \frac{\mathbf{k}^2 + m^2}{\beta(1-\beta)}$$

in the denominator in the right-hand side of Eq. (19) (in accordance with the definition of cross section (3) and relation (18) for q^2), where s_1 is the invariant mass squared of the created electron–positron pair in process (1) at $\mathbf{q} = 0$. In the numerator, we can neglect terms of the order of $\mathbf{q}^n$ with $n > 2$. In the region $\sigma < \mathbf{q}^2 < \infty$, we can use expression (19).

In region (25), gauge invariance requires the $\mathbf{q}^2$-dependence of the cross section to be of the form [14]

$$\frac{\mathbf{q}^2}{\left(\mathbf{q}^2 + m^2 s_1^2/s^2\right)^2}.$$

We can therefore perform elementary integration over $d\mathbf{q}$ in this region and over the azimuthal angle of the two-dimensional vector $\mathbf{k}$ and derive

$$\frac{d\sigma^s}{d\beta\, d\mathbf{k}^2} = \frac{2\alpha^3}{(m^2+\mathbf{k}^2)^2} \times \left(1 - 2\beta(1-\beta) + \frac{4\beta(1-\beta)m^2\mathbf{k}^2}{(m^2+\mathbf{k}^2)^2}\right) \times \left(\ln\frac{\sigma s^2\beta^2(1-\beta)^2}{m^2(m^2+\mathbf{k}^2)^2} - 1\right). \tag{26}$$

To obtain the electron (positron) spectrum in region (25), we have to integrate Eq. (26) over $d\mathbf{k}^2$. The result is

$$\frac{d\sigma^s}{d\beta} = 2\alpha r_0^2 \left\{\left(1 - \frac{4}{3}\beta(1-\beta)\right) \times \left(\ln\frac{\sigma s^2\beta^2(1-\beta)^2}{m^6} - 1\right) - 2 + \frac{26}{9}\beta(1-\beta)\right\}. \tag{27}$$

The total electron (positron) spectrum also contains a contribution from the region $\sigma < \mathbf{q}^2 < \infty$. To derive it, we integrate Eq. (20) over $\mathbf{q}^2$ and obtain

$$\frac{d\sigma^l}{d\beta} = 2\alpha r_0^2 \times \left[2 - \ln\frac{\sigma}{m^2} + 2\beta(1-\beta)\left(\frac{2}{3}\ln\frac{\sigma}{m^2} - \frac{13}{9}\right)\right]. \tag{28}$$

The electron spectrum in the case of the undetected recoil electron is the sum of $d\sigma^s/d\beta$ and $d\sigma^l/d\beta$, which is given by the well known expression

$$\frac{d\sigma}{d\beta} = 2\alpha r_0^2 \left(1 - \frac{4}{3}\beta(1-\beta)\right) \times \left(\ln\frac{s^2\beta^2(1-\beta)^2}{m^4} - 1\right). \tag{29}$$

It describes the corresponding differential cross section for e^+e^- pair production by a high-energy photon on an elementary electric charge. It is also suitable for pair production in the nonscreening Coulomb field (with the substitution $\alpha^3 \to \alpha^3 Z^2$).

If the recoil electron is not detected, we can also study the double distribution of the positron over the energy $\omega\beta$ and the perpendicular momentum $\mathbf{k}$, which are related to its scattering angle θ as $\theta = 2|\mathbf{k}|(\beta\sqrt{s})^{-1}$. For this, we have to integrate differential cross section (19) over $d\mathbf{q}$ in the region $\mathbf{q}^2 > \sigma$ and add the result to contribution (26) from the region $\mathbf{q}^2 < \sigma$. Such integration of the expression (19) gives

$$\frac{d\sigma^l}{d\beta\,d\mathbf{k}^2} = \frac{2\alpha^3}{(m^2+\mathbf{k}^2)^2} \times \times \left\{ 2\beta(1-\beta)\left(1-\frac{6m^2\mathbf{k}^2}{(m^2+\mathbf{k}^2)^2}\right) - - \left[1-2\beta(1-\beta)+\frac{4\beta(1-\beta)m^2\mathbf{k}^2}{(m^2+\mathbf{k}^2)^2}\right] \times \times \ln\frac{\sigma m^2}{(m^2+\mathbf{k}^2)^2}\right\}. \quad (30)$$

The term $\ln\left(\sigma m^2/(m^2+\mathbf{k}^2)^2\right)$ cancels in the total distribution, and we obtain

$$\frac{d\sigma}{d\beta\,d\mathbf{k}^2} = \frac{2\alpha^3}{(m^2+\mathbf{k}^2)^2} \times \times \left\{ 2\beta(1-\beta)\left(1-\frac{6m^2\mathbf{k}^2}{(m^2+\mathbf{k}^2)^2}\right) + + \left[1-2\beta(1-\beta)+\frac{4m^2\mathbf{k}^2\beta(1-\beta)}{(m^2+\mathbf{k}^2)^2}\right] \times \times \left(2\ln\frac{s\beta(1-\beta)}{m^2}-1\right)\right\}. \quad (31)$$

When integrating (31) with respect to $d\mathbf{k}^2$, the first term in the curly brackets vanishes and we come to spectrum (29). On the other hand, we can also integrate (31) over β and obtain

$$\frac{d\sigma}{d\mathbf{k}^2} = \frac{2\alpha^3}{3(m^2+\mathbf{k}^2)^2}\left[4\left(1+\frac{m^2\mathbf{k}^2}{(m^2+\mathbf{k}^2)^2}\right)\ln\frac{s}{m^2} - - \frac{29}{3} - \frac{44\,m^2\mathbf{k}^2}{3(m^2+\mathbf{k}^2)^2}\right]. \quad (32)$$

4. POLARIZATION OF THE CREATED ELECTRON

The created (fast) electron polarization in process (1) depends on all kinematic variables and at high energies can be written as

$$P(\beta,\mathbf{k},\,\mathbf{q}) = m\xi_2 \times \times \frac{T_{(\mu\nu)[\lambda\rho]}(e_{1\lambda}e_{2\rho}-e_{1\rho}e_{2\lambda})4\,p_\mu p_\nu d\Phi/q^4}{T_{(\mu\nu)(\lambda\rho)}(e_{1\lambda}e_{1\rho}+e_{2\lambda}e_{2\rho})4\,p_\mu p_\nu d\Phi/q^4}. \quad (33)$$

We note that we can eliminate the factor $d\Phi/q^4$ from this equation, but if our aim is, for example, to obtain the quantities $P(\beta,\mathbf{q})$, $P(\beta)$, and so on, then we have to first integrate both the numerator and the denominator over the corresponding variables and only then to take their ratio. It is obvious that the denominator is defined by the cross section and we have to investigate the numerator (or the part of the cross section that depends on the circular polarization of the photon and the longitudinal polarization of the created electron) in different experimental setups.

In terms of the invariants used, the numerator in Eq. (33) is expressed as (without the factor $d\Phi/q^4$)

$$16m\xi_2\left\{\left[\frac{(k_2p)}{\chi_1}-\frac{(k_1p)}{\chi_2}\right] \times \times \left[\frac{\chi_1+\chi_2}{\chi_1\chi_2}\big((k_2p)(kS)+\chi_1(pS)\big)-\frac{(kp)(k_2S)}{\chi_2}\right] + + \frac{q^2(\chi_2-\chi_1)(kp)(pS)}{2\chi_1\chi_2^2}\right\}. \quad (34)$$

We next use the covariant form of the electron polarization 4-vector, namely,

$$S = \frac{(kk_1)k_1 - m^2k}{m(kk_1)}. \quad (35)$$

It means that in the rest frame of the created electron, $S=(0,-\mathbf{n})$, where $\mathbf{n}$ is the unit vector along the photon 3-momentum.

The used invariants are expressed in terms of the Sudakov variables as

$$2m(pS) = s\left(1-\beta-\frac{m^2}{\chi_1}\right),$$

$$m(kS)=\chi_1, \quad m(k_2S) = (k_1k_2) - m^2\frac{\chi_2}{\chi_1},$$

and the expression in the braces in the right-hand side of Eq. (34) becomes very simple:

$$\frac{s^2q^2}{8\chi_2}\left[\frac{1-2\beta}{\chi_1}-\frac{m^2}{\chi_1}\left(\frac{1}{\chi_1}-\frac{1}{\chi_2}\right)\right].$$

We can now write the polarization-dependent part of the cross section

$$\frac{d\sigma_\xi}{d\beta\,d\mathbf{k}\,d\mathbf{q}} = -\frac{2\alpha^3\xi_2\mathbf{q}^2}{\pi^2q^4(m^2+\mathbf{k}^2)[m^2+(\mathbf{k}+\mathbf{q})^2]} \times \times \left[1-2\beta-2m^2\left(\frac{1-\beta}{m^2+(\mathbf{k}+\mathbf{q})^2}-\frac{\beta}{m^2+\mathbf{k}^2}\right)\right], \quad (36)$$

where, as in the unpolarized case, we have to set $q^4=\mathbf{q}^4$ in the region $\mathbf{q}^2>\sigma$ and $q^4=[\mathbf{q}^2+m^2s_1^2/s^2]^2$ in the region $\mathbf{q}^2<\sigma$.

For events with the scattered (or recoil) electron detected, we can integrate over $d\mathbf{k}^2$ and obtain the part of the double differential cross section in the simple form

$$\frac{d\sigma_\xi^l}{d\beta\,d\mathbf{q}} = \frac{4\alpha^3\xi_2(1-2\beta)}{\pi\mathbf{q}^4x^2}\big[\Psi_2-\Psi_1\big]. \quad (37)$$

We note that this distribution is antisymmetric under the replacement of β with $1-\beta$, whereas the polarization-independent part of the cross section (see Eq. (20)) is symmetric. Besides, at very small values of $\mathbf{q}^2$, cross section (37) does not depend on $\mathbf{q}^2$ due to the factor x^2 in the denominator, whereas cross section (20) has a pole at $\mathbf{q}^2 \to 0$. The last feature implies that the polarization-dependent part of the spectrum in the region $\mathbf{q}^2 < \sigma$ cannot have terms that contain the large logarithm $\ln(s/m^2)$ that arises in the case of a pole-like behavior as $\mathbf{q}^2 \to 0$.

The created electron polarization along the direction $-\mathbf{n}$, in its rest frame, is defined by the relation

$$P = \xi_2 P(\beta, \mathbf{q}^2) = d\sigma_\xi^l / d\sigma^l,$$

whence the polarization transfer coefficient is

$$P(\beta, \mathbf{q}^2) = \frac{(1-2\beta)\big(\Psi_2 - \Psi_1\big)}{x^2\big[(1-2\beta(1-\beta))\Psi_1 + 2\beta(1-\beta)\Psi_2\big]}. \quad (38)$$

The quantity $P(\beta, \mathbf{q}^2)$ is antisymmetric under $\beta \to 1-\beta$, and its magnitude is of the order of unity inside a wide region of the kinematic variables. This allows measuring even rather small values of circular polarizations.

If the scattered electrons are recorded by a narrow circular detector, we have to integrate over the detector aperture as described above in the unpolarized case. This procedure results in

$$P(\beta) = \frac{(1-2\beta)\big[D(z_0) - D(z_1)\big]}{A(z_0) - A(z_1) + \beta(1-\beta)\big[B(z_0) - B(z_1)\big]}, \quad (39)$$
$$D(z) = 2z[\operatorname{th}(z) - \operatorname{cth}(2z)].$$

If all recoil momenta with $l > l_0$ are recorded, then the polarization $P(\beta)$ can be derived with the same rules as described at the end of Sec. 3, namely, we have to eliminate $A(z_1)$, $B(z_1)$, and $D(z_1)$ from Eq. (39) and use $l_0 = 2m \operatorname{sh} z_0$. If the angular distribution of the recoil electron is measured, then we have to use $\operatorname{sh} z = \operatorname{ctg} \vartheta$.

We now consider the experimental setup without detection of the scattered (or recoil) electron. Our goal is to obtain the double distribution of the created electron polarization $P(\beta, \mathbf{k}^2)$ and the spectrum-like one $P(\beta)$ by analogy with Eqs. (38) and (39). Besides, we can also investigate the corresponding distribution over $\mathbf{k}^2$. In these cases, we must take the contributions of both regions $\mathbf{q}^2 > \sigma$ and $\mathbf{q}^2 < \sigma$ into account.

Integrating the right-hand side of Eq. (36) with respect to $d^2\mathbf{q}$ over the region $\mathbf{q}^2 > \sigma$ and the azimuthal angle of $\mathbf{k}$ gives

$$\frac{d\sigma_\xi^l}{d\beta\, d\mathbf{k}^2} = \frac{2\alpha^3 \xi_2 (\mathbf{k}^2 - m^2)}{(m^2 + \mathbf{k}^2)^3} \times \left[\ln \frac{\sigma m^2}{(m^2 + \mathbf{k}^2)^2}(1 - 2\beta) + 2(1 - \beta)\right]. \quad (40)$$

We see that this part of the cross section has no definite symmetry under $\beta \to 1 - \beta$. The corresponding contribution of the region $\mathbf{q}^2 < \sigma$ is

$$\frac{d\sigma_\xi^s}{d\beta\, d\mathbf{k}^2} = \frac{2\alpha^3 \xi_2 (\mathbf{k}^2 - m^2)(1 - 2\beta)}{(m^2 + \mathbf{k}^2)^3} \times \left(1 - \ln \frac{\sigma s^2 \beta^2 (1 - \beta)^2}{m^2 (m^2 + \mathbf{k}^2)^2}\right). \quad (41)$$

In the sum of (40) and (41), the auxiliary parameter σ cancels in the same manner as it did for the unpolarized part of the cross section, and we have

$$\frac{d\sigma_\xi}{d\beta\, d\mathbf{k}^2} = \frac{2\alpha^3 \xi_2 (\mathbf{k}^2 - m^2)}{(m^2 + \mathbf{k}^2)^3} \times \left\{\left(1 - 2\ln \frac{s\beta(1-\beta)}{m^2}\right)(1-2\beta) + 2(1-\beta)\right\}. \quad (42)$$

We can now write the total distributions over β and over $\mathbf{k}^2$. Elementary integrations give

$$\frac{d\sigma_\xi}{d\beta} = 0, \quad \frac{d\sigma_\xi}{d\mathbf{k}^2} = \frac{2\alpha^3 \xi_2 (\mathbf{k}^2 - m^2)}{(m^2 + \mathbf{k}^2)^3}. \quad (43)$$

Having different distributions for both polarization-dependent and polarization-independent parts of the cross section, we can define the respective polarizations of the created electron $P(\beta)$, $P(\mathbf{k}^2)$, and $P(\beta, \mathbf{k}^2)$, by taking the corresponding ratios. We first note that $P(\beta)$ goes to zero because $d\sigma_\xi / d\beta = 0$. The polarization $P(\mathbf{k}^2)$, which is the ratio of the right-hand sides of Eqs. (43) and (32) without the factor ξ_2, decreases logarithmically as the photon energy increases because $d\sigma_\xi / d\mathbf{k}^2$ does not contain a logarithmic contribution. The polarization $P(\beta, \mathbf{k}^2)$ (the ratio of the right-hand sides of Eqs. (42) and (31)) at very high energies tends to the limit that is independent of energy,

$$P(\beta, \mathbf{k}^2)|_{s\to\infty} = \frac{(m^4 - \mathbf{k}^4)(1 - 2\beta)}{(m^2 + \mathbf{k}^2)^2 - 2\beta(1-\beta)(m^4 + \mathbf{k}^4)}. \quad (44)$$

The quantity $P(\beta)$ vanishes (with the accuracy of m/ω) if we take all events with $0 < \mathbf{k}^2 < \infty$ into account. But eliminating the region of very small values of $\mathbf{k}^2$ increases (in absolute value) the number of events that depend on the photon circular polarization and decreases the unpolarized event number. Therefore, the created-electron polarization can be determined with high efficiency by the spectrum distribution of the created electron (or positron) using the constraint

$$\mathbf{k}^2 > \mathbf{k}_0^2$$

on the event selection, where $\mathbf{k}_0^2$ is of the order of a few m^2. This constraint means that events with very

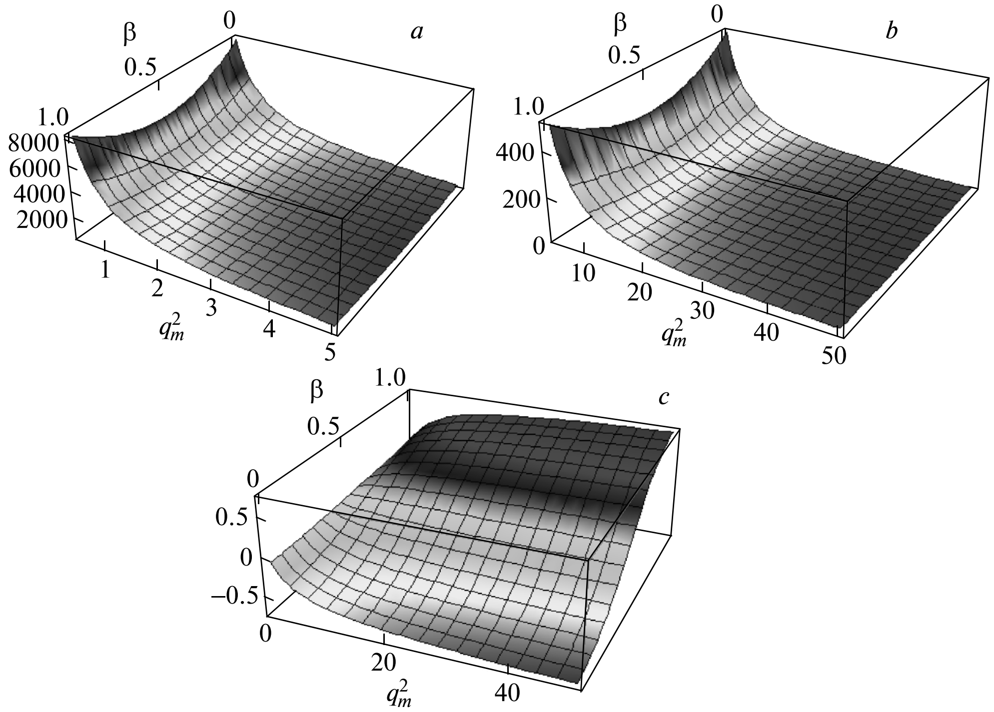

Fig. 2. (a,b) Double differential cross section defined in Eq. (20) and (c) the respective distribution for the electron polarization given by Eq. (38). The energy fraction of the electron is $\omega(1-\beta)$ and $q_m^2 = \mathbf{q}^2/m^2$

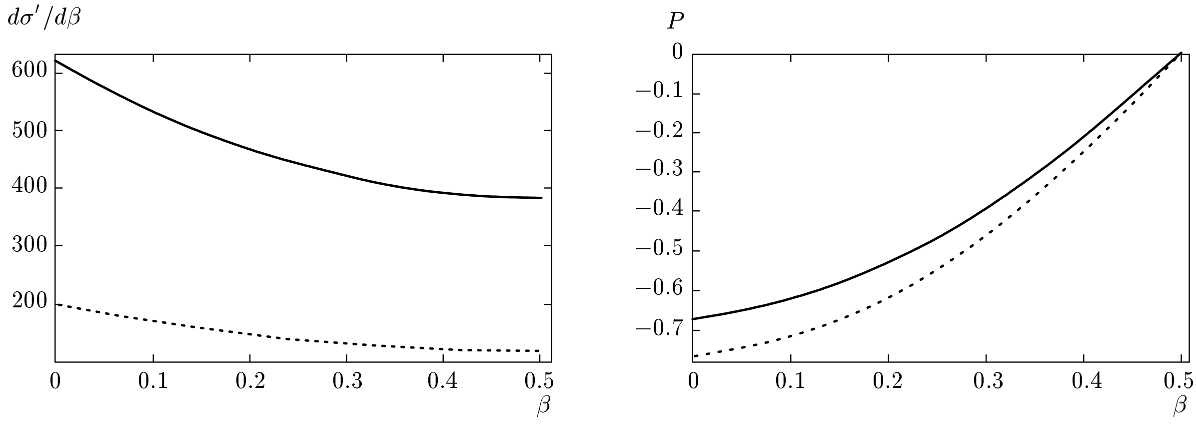

Fig. 3. The unpolarized part of the cross section and polarization of the created electron given by Eqs. (22) and (39) in the reaction c.m.s. (with $z_0 = \mathrm{Arsh}(\theta_{min}E/2m)$ and $z_1 = \mathrm{Arsh}(\theta_{max}E/2m)$) at $E = 100$ MeV for events with the minimal electron scattering angles $\theta_{min} = 1^\circ$ (solid curves) and $\theta_{min} = 2^\circ$ (dotted curves), and with $\theta_{max} = 6^\circ$ in both cases

small angles of the created electron and positron are excluded.

A simple calculation gives the electron polarization in such an experimental setup in the form

$$P(\beta, \mathbf{k}_0^2) = \frac{y(1+y)A(s,\beta)}{B(y,s,\beta)}, \quad y = \frac{\mathbf{k}_0^2}{m^2}, \qquad (45)$$

where

$$A(s,\beta) = 2(1-\beta) + \left(1 - 2\ln\frac{s\beta(1-\beta)}{m^2}\right)(1-2\beta),$$

$$B(y,s,\beta) = \left[(1+y)^2 - \frac{2}{3}\beta(1-\beta)(2+3y+3y^2)\right] \times$$
$$\times\, 2\ln\frac{s\beta(1-\beta)}{m^2} - (1+y)^2 + \frac{4}{3}\beta(1-\beta)(1+3y^2).$$

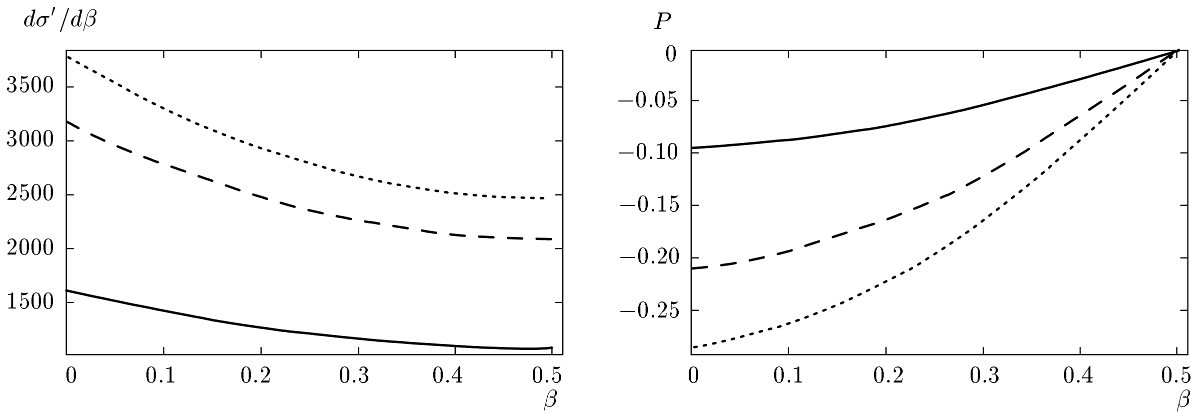

Fig. 4. The same as in Fig. 3 but for events in the rest frame of the initial electron with $z_0 = \mathrm{Arsh}(\mathrm{ctg}\,\vartheta_{max})$ and $z_1 = \mathrm{Arsh}(\mathrm{ctg}\,\vartheta_{min})$ in Eqs. (22) and (39). We use $\theta_{max} = 75^\circ$ and $\theta_{min} = 60^\circ$ (solid lines), 30° (dashed lines), and 5° (dotted lines)

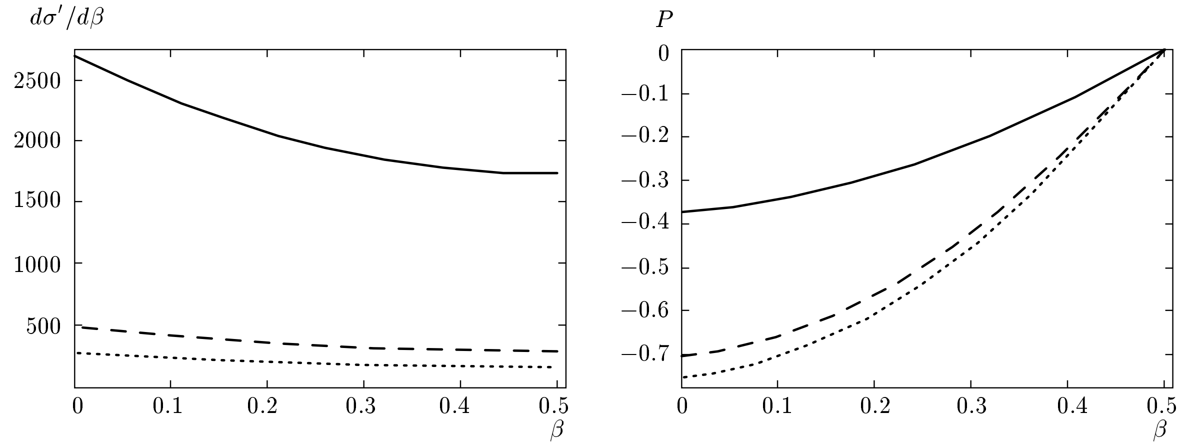

Fig. 5. The same as in Fig. 4 but at $z_0 = \mathrm{Arsh}(l_0/m)/2$ and $A(z_1) = B(z_1) = D(z_1) = 0$ in Eqs. (22) and (39); $l_0 = m$ (solid curves), $10\,m$ (dashed curves), $20\,m$ (dotted curves)

5. NUMERICAL RESULTS AND DISCUSSIONS

In this section, we demonstrate some numerical estimates for the created-electron polarization (along the photon 3-momentum direction in the rest frame) for different experimental situations. Together with polarizations, we show the corresponding unpolarized parts of the cross section for which we always use units μb or $\mu\mathrm{b/MeV}^2$. The results for different experimental setups with detection of the recoil (or scattered) electron are shown in Figs. 2–5 and those without detection, in Figs. 6–8. All curves in these figures are correct when the condition $s \gg \mathbf{q}^2, \mathbf{k}^2, m^2$ is satisfied, and we assume that the minimal value of the recoil 3-momentum is always of the order of m. In this case, different unpolarized differential cross sections are symmetric under the change $\beta \to 1-\beta$, whereas the polarizations are antisymmetric.

We note that all curves in Figs. 2, 4, 5 are independent of the collision energy (only the above-mentioned constraints on the values of $s, \mathbf{q}^2$, and m^2 are supposed to hold), and the curves in Fig. 3 depend on energy. The reason is that in Fig. 3, we give the corresponding distributions for events in the c.m.s. with fixed scattered-electron angles (but not $\mathbf{q}^2$). Within the used accuracy, these angles are expressed via the perpendicular transferred momentum and the initial electron energy by the simple relation $\mathbf{q}^2 = \theta^2 E^2$, $E = \sqrt{s}/2$. It means that at a fixed θ, the value of $\mathbf{q}^2$ increases as the energy squared, but, as follows from Fig. 2, the cross section decreases very rapidly as $\mathbf{q}^2$ increases.

To estimate the energy dependence of the curves in

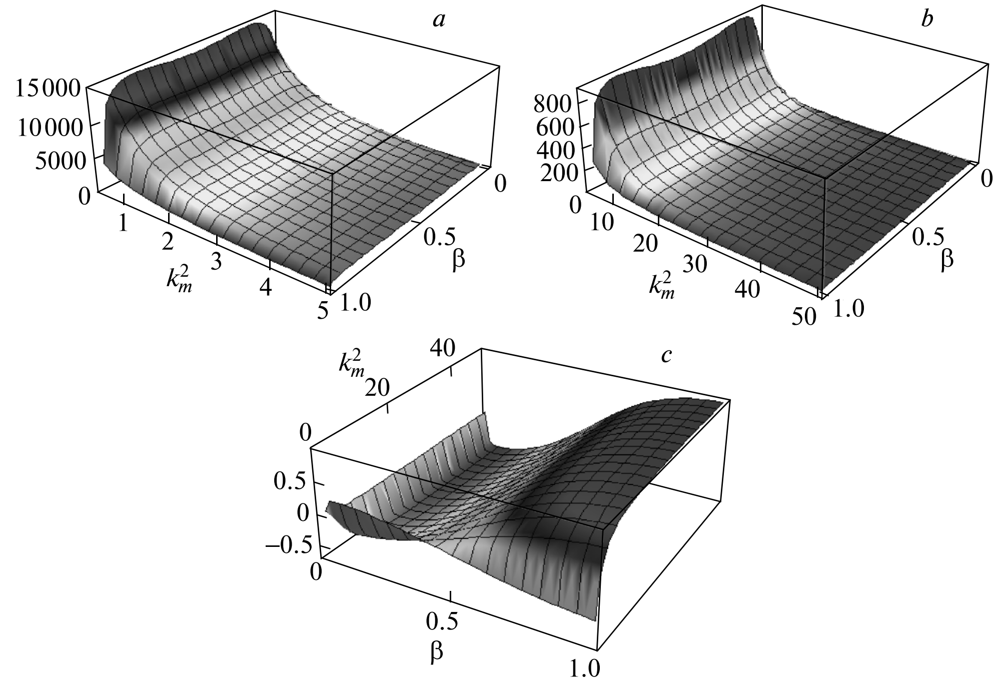

Fig. 6. (a,b) Double differential cross section defined by Eq. (31) and (c) the respective distribution for the electron polarization that is the ratio of the right-hand side of Eq. (42) at $\xi_2 = 1$ to cross section (31), at $s = 300$ MeV^2 with $k_m^2 = \mathbf{k}^2/m^2$

Fig. 3, we perform the corresponding calculations also at $E = 1$ GeV and 10 GeV and observe that polarization is practically independent of energy, whereas the cross section loses more than three orders of magnitude as the energy increases from 100 MeV to 10 GeV.

An entirely different picture of the angular distribution of recoil electrons is observed for events in the rest frame. In this case, the relation between the scattering angle and the perpendicular transferred momentum does not contain the collision energy. Therefore, the curves in Fig. 4 are the same at the above-mentioned energies. Because

$$\mathbf{q}^2 = 4m^2 \operatorname{ctg}^2 \theta$$

in the rest frame, the cross section decreases as the recoil electron scattering angle θ increases.

In Fig. 5, to complete the description of events with the recorded scattered (or recoil) electron, we also give the unpolarized cross section and polarization at different values of the minimal magnitude of the recoil electron 3-momentum.

As regards the experimental setup without detection of the recoil (or scattered) electron, the corresponding events, by definition, include all values of $\mathbf{q}^2$ starting from zero. In this case, the dependence of the differential cross section $d\sigma/d\beta\, d\mathbf{k}\, d\mathbf{q}$ on the collision energy arises due to the $1/q^4$ factor in Eq. (3). After the integration of the cross section with respect to $d\mathbf{q}$, this dependence leaves a trace as a term enhanced by the logarithmic factor in Eq. (31). This integrated cross section is said to increase logarithmically as the energy increases.

In Fig. 7, we show the differential cross section and polarization of the electron as functions of the positron perpendicular momentum only. As noted above, the cross section increases logarithmically with energy, whereas the polarization decreases. The polarization can nevertheless be measured using such a distribution up to energies $s = 1$ GeV^2 because the corresponding event number is sufficiently large. A more advantageous situation occurs when events with $0 < \mathbf{k}^2 < \mathbf{k}_0^2$ are excluded and the polarization increases with the collision energy (as it is demonstrated in Fig. 8). The unpolarized cross section is not given in this figure, but can be derived by integrating cross section (31) with respect to $\mathbf{k}^2$ from $\mathbf{k}_0^2$ up to ∞.

We compare our approach and the obtained results with the corresponding investigations in Ref. [12]. We first note that in both papers, only the Borselino diagrams are taken into account for theoretical de-

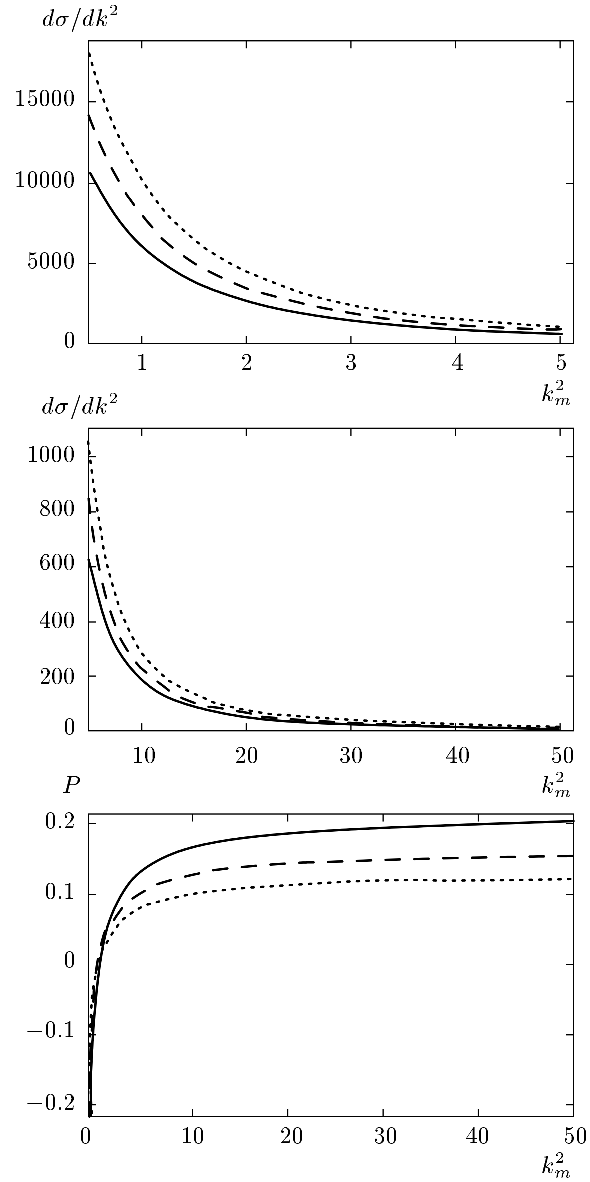

Fig. 7. Differential cross section defined by Eq. (32) and the corresponding polarization, which is the ratio of the right-hand side of Eq. (43) at $\xi_2 = 1$ to cross section (32), at $s = 100$ MeV^2 (solid curves), 300 MeV^2 (dashed curves), 1 GeV^2 (dotted curves)

scription of process (1) and the Sudakov variables are used. In Ref. [12], the polarization of both components of the created pair is considered, but we concentrated on the polarization of the fast electron only. In Ref. [12], the calculations were performed in the leading logarithmic approximation using the equivalent-photon method, whereas our results also include a contribution that does not depend on energy. We consider different event selections, particularly distributions over the recoil-electron variables, which cannot be studied by the method used in Ref. [12].

We must therefore compare formula (14) in Ref. [12] with the coefficient at $\ln(s/m^2)$ in our unpolarized (Eq. (26)) and polarized (Eq. (41)) cross sections caused by small values of $\mathbf{q}^2 < \sigma$. We see that our unpolarized cross section is twice the one in Ref. [12]. This means that we perform the spin summation. We also use the polarized cross section, which should be twice the one in Ref. [12] (if we set $\xi = \lambda$ and $\delta_- = 1$). But we see that this is not so. The reason is that our parameterization for the electron polarization 4-vector (see Eq. (35)) is different from the one in Eq. (12) in Ref. [12]. Let $\tilde{S}$ be the polarization 4-vector used in Ref. [12]. Then in our notation, we have

$$2m(p\tilde{S}) = s(1-\beta), \quad m(k\tilde{S}) = \chi_1 - \frac{m^2}{1-\beta},$$

$$m(k_2\tilde{S}) = (k_1k_2) - \frac{m^2\beta}{1-\beta}.$$

These relations are different from the corresponding ones with the 4-vector S instead of $\tilde{S}$ (see formulas after Eq. (35)). Just this difference is the source of different forms of the polarization-dependent parts of differential cross sections. We also note that in accordance with Eq. (43), our spectral distribution vanishes for both contributions, the leading logarithmic and constant ones, whereas the logarithmic contribution is nonzero in Ref. [12] (Eq. (16)).

The unpolarized cross section, within the adopted accuracy, is symmetric under the change $\beta \rightleftarrows 1-\beta$. With our choice of the 4-vector S, the created-electron polarization is antisymmetric if the recoil (or scattered) electron is recorded. Otherwise, there are nonlogarithmic contributions that have no definite symmetry under this change (see Eqs. (42) and (45)).

The accuracy of our calculations is restricted by neglected terms of the order of m^2/s and by the radiative corrections. The former can be essential near the boundaries of the electron spectrum [8], and therefore our calculations are valid in the region $0.1 < \beta < 0.9$. As regards the radiative corrections, they violate the above-mentioned symmetries at the level of several percent in this region of electron energies, at least for unpolarized events, due to the possibility of a hard photon emission [17].

6. CONCLUSION

The process of e^+e^--pair production in the scattering of a circularly polarized photon beam on electrons gives rise to polarization of the produced electron and

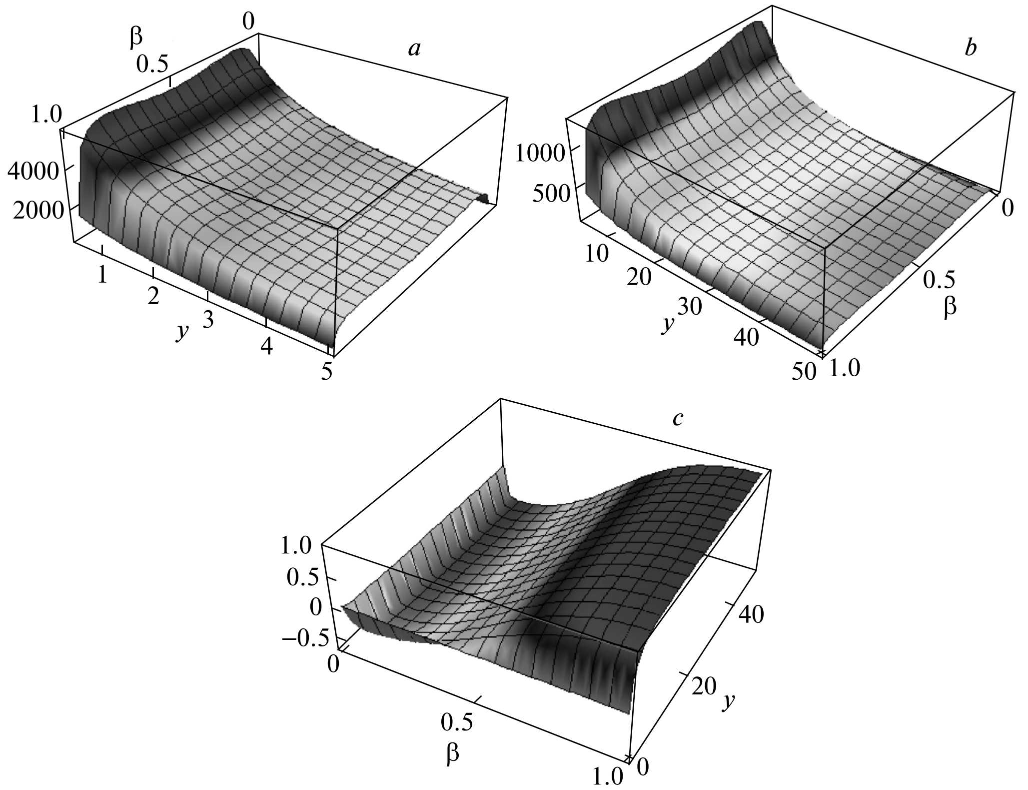

Fig. 8. (a,b) Differential cross section and (c) the created-electron polarization (Eq. (45)) as functions of the energy fraction β and the parameter y at $s = 300$ MeV^2

positron. At high energy of the photon beam, this effect can be used both for the production of high-energy polarized electrons (and positrons) (see Ref. [12]) and for the measurement of the photon circular polarization degree, because the differential cross section and polarization transfer coefficient do not decrease as the photon energy increases. The leading contribution to these physical quantities is made by events with small transferred momenta squared ($|q^2|/s \ll 1$), when the e^+e^- pair carries away all the photon energy. This contribution is determined by the Borselino diagrams (Fig. 1).

We calculated this contribution for different distributions of the final particles using the technique of Sudakov variables. We considered two essentially different physical situations. The first one is concerned with the detection of not only the produced electron but also the scattered (recoil) electron. That kind of detection is quite possible because the final electrons belong to different (nonoverlapping) phase-space regions. The results of our numerical calculations are presented in Figs. 2–5 in the case where the minimal transverse transferred momentum is of the order of the electron mass ($|\mathbf{q}^2|_{min} \approx m^2$).

The typical differential cross sections turn out to be of the order of 1 mb and the polarization transfer coefficients are of the order of unity and are antisymmetric under the replacement $\beta \to 1 - \beta$. Our calculations imply integration over the entire interval of the electron azimuthal angles. In principle, they can be done for any detector geometry because the differential cross section (the formulas (19) and (36)) is easy to integrate numerically.

The results of calculations in the case where the scattered electron is not detected are presented in Figs. 6–8. In these calculations, the contributions of all events with $|\mathbf{q}^2| \geq 0$ are added. The differential cross sections (formulas (31) and (42)) acquire a contribution that increases logarithmically with energy. At the cost of this, the cross sections turn out to be somewhat larger than in the first case. The polarization transfer coefficient is also of the order of unity if the electron energy is measured, but is essentially smaller if the integration over energy is done in the entire range of values (Fig. 7). It is important to note that such an experimental setup is possible in the interaction of photons with an electron beam because during the interaction of photons with matter, scattering on the atomic electrons with e^+e^--pair production (without the recoil electron detection) is only a background process relative to the Bethe–Heitler process.

The authors thank A. Glamazdin for the useful discussion.

REFERENCES

1. V. F. Boldyshev and Yu. P. Peresunko, Yad. Fiz. **14**, 1027 (1971); **19**, 144 (1974).
2. E. A. Vinokurov and E. A. Kuraev, Zh. Eksp. Theor. Fiz. **62**, 1142 (1973).
3. E. A. Vinokurov and N. P. Merenkov, Yad. Fiz. **21**, 781 (1975).
4. V. F. Boldyshev, E. A. Vinokurov, N. P. Merenkov, and Yu. P. Peresunko, Phys. Element. Particles Atom. Nuclei **25**, 696 (1994).
5. I. Endo, S. Kasai, M. Harada et al., Nucl. Instr. Meth. A **280**, 144 (1989).
6. E. Haug, Phys. Rev. D **31**, 2120 (1985); D **32**, 1594 (1985).
7. A. Borselino, Nuovo Cim. **4**, 112 (1947).
8. I. V. Akushevich, H. Anlauf, E. A. Kuraev et al., Phys. Rev. A **61**, 032703 (2000).
9. A. S. Arichev, A. P. Potylitsin, and M. N. Strikanov, arXiv:0112060[ph].
10. G. L. Kotkin, V. G. Serbo, and V. I. Telnov, Phys. Rev. ST — Accel. and Beams **6**, 011001 (2003).
11. A. I. Akhiezer and V. B. Berestetsky, *Quantum Electrodynamics*, Nauka, Moscow (1969).
12. V. V. Bytev, E. A. Kuraev, M. V. Galinsky, and A. P. Potylitsin, Pisma Zh. Eksp. Teor. Fiz. **75**, 542 (2002).
13. V. A. Khoze, M. I. Konchatnij, N. P. Merenkov et al., Europ. Phys. J. C **25**, 1999 (2002); H. Czyż, A. Grzelinska, J. H. Kühn, and G. Rodrigo, Europ. Phys. J. C **47**, 617 (2006); A. Denig, Nucl. Phys. Proc. Suppl. **162**, 81 (2006).
14. V. V. Sudakov, Zh. Eksp. Teor. Fiz. **30**, 87 (1956); V. G. Gorshkov, Usp. Fiz. Nauk **10**, 45 (1973).
15. C. Weizsäcker, Zs. Phys. **88**, 612 (1934); E. Williams, Phys. Rev. **45**, 729 (1934).
16. K. S. Suh and H. A. Bethe, Phys. Rev. **115**, 672 (1959).
17. E. A. Vinokurov, E. A. Kuraev, and N. P. Merenkov, Zh. Eksp. Teor. Fiz. **66**, 1916 (1974).